Received: 28 May 2018 | Revised: 13 March 2019 | Accepted: 20 May 2019
DOI: 10.4218/etrij.2018-0249

ORIGINAL ARTICLE

ETRI Journal WILEY

Analysis of adjacent channel interference using distribution function for V2X communication systems in the 5.9-GHz band for ITS

Yoo Seung Song | **Shin Kyung Lee** | **Jeong Woo Lee** | **Do Wook Kang** | **Kyoung Wook Min**

Artificial Intelligence Research Laboratory, Electronics and Telecommunications Research Institute, Daejeon, Rep. of Korea

Correspondence
Yoo Seung Song, Artifical Intelligence Research Laboratory, Electronics and Telecommunications Research Institute, Daejeon, Rep. of Korea.
Email: yssong00@etri.re.kr

Funding information
This work was supported by the ICT R&D program of MSIP/IITP (201500275, High Speed V-Link Communication Technology Development for Real Time Control of Autonomous Driving Vehicle, and 2018-0-00327, Development of Fully Autonomous Driving Navigation AI Technology in High-precision Map Shadow Environment).

Many use cases have been presented on providing convenience and safety for vehicles employing wireless access in vehicular environments and long-term evolution communication technologies. As the 70-MHz bandwidth in the 5.9-GHz band is allocated as an intelligent transportation system (ITS) service, there exists the issue that vehicular communication systems should not interfere with each other during their usage. Numerous studies have been conducted on adjacent interfering channels, but there is insufficient research on vehicular communication systems in the ITS band. In this paper, we analyze the interference channel performance between communication systems using distribution functions. Two types of scenarios comprising adjacent channel interference are defined. In each scenario, a combination of an aggressor and victim network is categorized into four test cases. The minimum requirements and conditions to meet a 10% packet error rate are analyzed in terms of outage probability, packet error rate, and throughput for different transmission rates. This paper presents an adjacent channel interference ratio and communication coverage to obtain a satisfactory performance.

KEYWORDS
ACI, C-ITS, coexistence, C-V2X, DSRC, LTE, PC5, V2X, WAVE

1 | INTRODUCTION

Automobiles are becoming smart mobile systems that offer convenience and safety to drivers by providing automated driving, infotainment, and road traffic information instead of simple transportation systems. An automated driving system is classified into four or five stages according to the functions and roles of the vehicle. Various events and situations occurring on a road are detected by mounted-sensors or delivered by the vehicle-to-anything (V2X) communication devices. The traffic information is provided to the driver if necessary or used for autonomous driving [1,2]. Use cases comprising V2X communication technologies and the message formats supporting them are published through standard documents [3–7]. Currently, V2X applications are becoming increasingly advanced and diversified as vehicular communication technologies are evolving.

Wireless access in vehicular environments (WAVE) and long-term evolution (LTE) are the key technologies in V2X communication in the unlicensed 5.9-GHz band for an intelligent transportation system (ITS) [8]. WAVE is a short-range wireless communication technology that supports V2X in a high-speed driving vehicle environment and follows the IEEE802.11 standard as well as the IEEE802.11p, which is a physical layer for vehicle radio access. This includes the IEEE1609.x series for security, networking, and multi-channel support, and this is the only V2X communication technology currently available for deployment [9–12]. WAVE technology performance has been verified through several projects and pilot services in the US, Europe, and Korea. 3rd Generation Partnership Project (3GPP) has recently standardized LTE Release 14 for cellular V2X (C-V2X) technology that is capable of inter-vehicle communication and continues to standardize 5G technologies to meet the objectives of a peak data rate of 20 Gbps, mobility of 500 km/h, latency of 1 ms, connection density of 10^6/km^2, five times spectrum efficiency, and user experienced data rate of 1 Gbps [13–15].

Recently, as shown in Figure 1, both V2X using WAVE and C-V2X using LTE have been demonstrated as network solutions for ITS service in the 5.9-GHz band. The WAVE system uses V2X technology to deliver information between the Road Side Unit (RSU) and vehicle using vehicle-to-infrastructure (V2I) and between two vehicles, whereas LTE provides the same service as WAVE through the PC5 interface including vehicle-to-pedestrian (V2P) and connects to a cellular network called evolved Node B through the Uu interface using vehicle-to-network (V2N). WAVE technology has MAC/PHY (medium access control/physical layer) characteristics that are advantageous for short-range wireless communication such as ad hoc communication. LTE technology is superior to long-distance wireless communication owing to its technical features that can restore signals at a lower level. Therefore, it can be stated that WAVE and LTE are mutually complementary. In addition, the technical verification of WAVE technology has been completed through various pilot projects, and WAVE technology is currently in the process of commercialization; however, it has the disadvantage of significantly large infrastructure construction costs. However, LTE can use the existing infrastructure to a certain extent, although the greatest problems are securing technologies until the commercial stage and a lack of verification testing. Currently, the US, Europe, and South Korea have announced the use of the 70-MHz band from 5.855 GHz to 5.925 GHz for an ITS service, which can cause the problem of adjacent channel interference (ACI) when both WAVE and LTE share this band. The radio frequency (RF) requirements between the two heterogeneous networks should be satisfied to avoid interference between them. The same ACI problem can occur between homogeneous

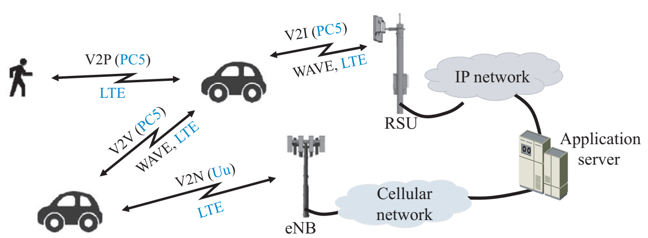

FIGURE 1 Coexistence of two V2X communication networks for ITS services

communication systems. This paper presents an analysis of the RF requirements for solving the ACI problems.

Recently, several studies have been conducted to solve the problem of ACI mainly for the LTE system. Among the studies conducted on ACI within an LTE network, Son and Kim [16] show that an adjacent channel interference ratio (ACIR) of at least 46 dB is required to prevent the occurrence of interference between the uplink channel from a mobile station and the downlink channel from a base station. To secure the reliability between vehicle-to-vehicle (V2V) communication devices using LTE, it has been proposed that the interference can be reduced through the scheduling of the resource block, transmission power, and modulation scheme as described in [17]. In both wireless local area network (LAN) and LTE environments, the same interference channel problem exists. The throughput capacity is improved by the scheduling algorithm using non-overlapping channels, power tuning, and partially overlapping channels, as described in [18]. Research [19] has been conducted to improve the throughput of the entire network by employing an effective downlink scheduling algorithm when LTE and dedicated short-range communication (DSRC) networks are used together for V2V and vehicle-to-infrastructure (V2I) communications. The ACI model was studied in [20] by simulating the channel interference between the service channel and the control channel according to the number of vehicles in a multichannel vehicular ad hoc networks environment.

By examining studies on ACI between LTE systems and heterogeneous systems, a mutual frame synchronization scheme and a new uplink scheduling scheme that coexist with TD-LTE and WiMAX systems are proposed in [21]. A performance enhancement was demonstrated in [22] using smart antenna beamforming techniques and guard bands to resolve the channel interference between M-WiMAX TDD and WCDMA FDD systems. Taking into consideration various interference factors, the beamforming schemes for maximizing the data rate and providing the required signal-to-noise ratio for high-mobility users have been studied in [23,24]. In [25], a risk-informed interference assessment was conducted to solve the frequency-sharing problem of Wi-Fi in an unlicensed band. In [26], the authors showed that the appropriate antenna setting and filtering techniques are effective in solving the channel interference problem of a TV receiver caused by the coexistence of a digital video broadcasting-terrestrial network. In addition, unsolved technical coexistence problems in the 5-GHz band observed in a network combination scenario analysis are mentioned in [27], including mobile edge computing, latency, and cross-frequency scheduling issues under a coexistence between LTE and DSRC systems. In the study by Voicu and others [25], the outage probability for the LTE downlink was analyzed using the proposed ACI model when IEEE 802.11C causes ACI to the LTE system.

An accurate ACI model is required when analyzing the performance of ACI through a numerical analysis or simulation. The ACI model derivation and performance analysis has been presented in [16,23,28–37]. Firstly, in the study of the ACI model using the distribution functions [16,29], the signal-to-interference-plus-noise ratio (SINR) equation was obtained by considering the co-channel and adjacent channel interference signals from multiple terminals using the same LTE network, and the ACI model was derived by using the probability density function (PDF) that was derived from the SINR equation. In order to solve the error problem of the PDF formula using the lognormal distribution when the difference in the distance between the desired path and the interference signal path is large, Kim and otherds [28] presented a method of assigning appropriate weights to each PDF by dividing the radius. In the study by Heath [30], the ACI model is derived using the Poisson point process for co-channel interference signals using the Gamma distribution with second-order moment matching. However, there was no study on various communication performance analysis including ACI model and throughput performance in heterogeneous networks between LTE and WAVE networks. Secondly, the ACI model that takes into consideration the channel characteristics was studied. In Kim et al's., study, the channel attenuation characteristics and channel rejection factor were considered for deriving the interference signal model. In [32–34], the leakage power of the adjacent channel was calculated by numerically analyzing the spectral mask characteristics of the transmitter and receiver and the frequency response of the filter for deriving the ACI factor. Lastly, considering the mutual characteristics of heterogeneous networks, [23,35,36] applied the ACI model while taking into consideration the interfering time, transmission period, and MAC scheme in the co-channel and adjacent channels as well as the characteristics of the interference channel. To improve the path loss model as well as the ACI model, [37] proposed the application of the optimal parameters to the path loss model according to the distance between the transmitter and receiver.

Thus far, there has been a lack of ACI research related to the coverage and distribution of the desired and interfering V2X signals in the 5.9-GHz band for ITS. The communication range changes depending on various use cases and communication environments. Therefore, the interference analysis is important when adjacent channels have various communication ranges. In this study, we analyze the performance based on the communication range, distribution, and RF characteristics of vehicles existing in two adjacent channels. The ACI system modeling is described in Section 2, and the PDF for the system modeling is derived in Section 3. The performance of the V2X communication system with ACI is analyzed in Section 4. Finally, some concluding remarks are presented in Section 5.

2 | SYSTEM MODELING

Two ACI scenarios are defined for the analysis. The first scenario, called the V2V ACI scenario, is when one aggressor V2V channel causes ACI in a victim V2V channel, as shown in Figure 2. The desired V2V communication link is made using the f_1 channel at a distance of d_1 from the transmitter, whereas the interfering V2V link is made using the f_2 channel at a distance of d_2 from the victim.

The second scenario, called the (infrastructure-to-vehicle) I2V ACI scenario, comprises a victim I2V channel that is interfered with by an aggressor V2V channel, as shown in Figure 3. The desired I2V link communicates with the f_1 channel at a distance of d_1 from the RSU, whereas the interfering V2V link communicates with the f_2 channel at a distance of d_2 from the victim.

As shown in Figure 4, the victim vehicle not only receives a signal from the assigned channel but also experiences interference from the adjacent channel owing to the imperfection of both the aggressor transmitter mask and the victim receiver filter. The former interference signal, referred to as the adjacent channel leakage ratio (ACLR), is defined as the ratio of the transmitted power to the power measured in the adjacent channel. The latter, called adjacent channel selectivity (ACS), is defined as the ratio of the receiver filter attenuation on the assigned channel to that on the adjacent channel. The overall evaluated system performance is represented by the ACIR, which is defined

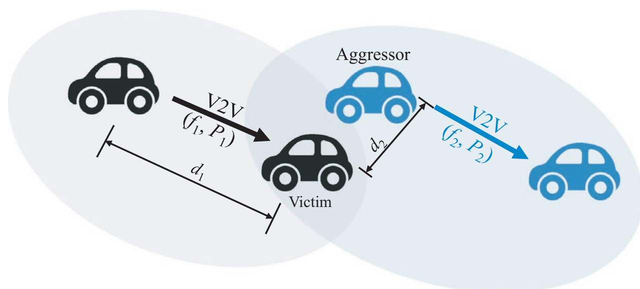

FIGURE 2 V2V ACI scenario wherein an aggressor V2V channel interferes with a victim V2V channel

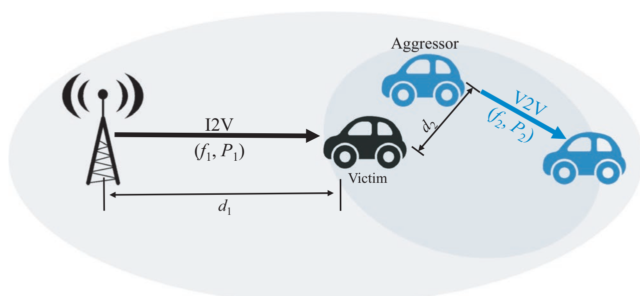

FIGURE 3 I2V ACI scenario wherein I2V and V2V channels are causing mutual ACI

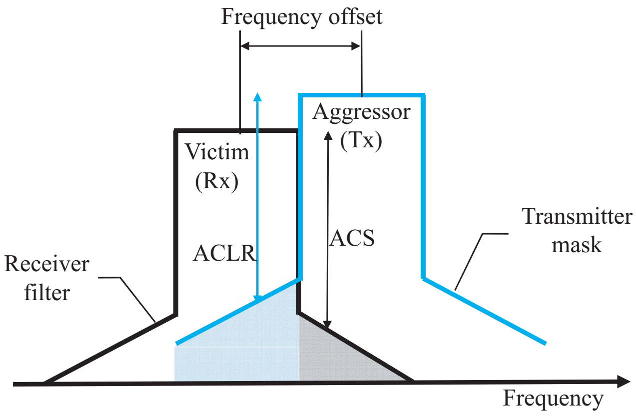

FIGURE 4 ACIR resulting from transmitter and receiver imperfections

as the ratio of the total power from the assigned channel to the total interference power affecting a victim vehicle, which results from transmitter and receiver imperfections. The ACIR can be obtained from the ACLR and ACS as follows:

$$\mathrm{ACIR} \triangleq \phi = \frac{1}{1/\mathrm{ACLR} + 1/\mathrm{ACS}}. \tag{1}$$

In this paper, an ACI analysis is conducted for 10-MHz channels such that the bandwidth of all the channels and the offset between the channels is equal to 10 MHz.

3 | DERIVATION OF SINR DISTRIBUTIONS

Based on the system modeling and the considered scenarios, the PDF of the received signal-to-interference-plus-noise ratio (SINR) is derived when the transmitted signal from the adjacent channel affects the signal reception of the victim vehicle.

For simplicity, the communication radius is assumed to have a circular cell structure. The victim vehicle is uniformly distributed within the communication range of the desired transmitter and has a distance d_1, whereas the aggressor vehicle is uniformly distributed within the communication range of the victim vehicle and has a distance d_2. Based on the given conditions, the SINR of the victim vehicle, denoted as γ, can be expressed as:

$$\gamma = \frac{P_{\mathrm{rx}}^{\mathrm{des}}}{N_0 + P_{\mathrm{rx}}^{\mathrm{agg}}}, \tag{2}$$

where $P_{\mathrm{rx}}^{\mathrm{des}}$ and $P_{\mathrm{rx}}^{\mathrm{agg}}$ are the received signal power from the desired transmitter and the aggressors, respectively, and N_0 is the noise density in *W/Hz*.

In general, the noise power is negligible as compared to the ACI, and on considering the transmitted power and path loss, the SINR can be re-written as:

$$\begin{aligned}\gamma &\approx \frac{A_1 d_1^{-\alpha_1} \cdot 10^{P_{\mathrm{tx}}^{\mathrm{des}}/10}}{A_2 d_2^{-\alpha_2} \cdot 10^{P_{\mathrm{tx}}^{\mathrm{agg}}/10} \cdot 10^{-\phi^{\mathrm{agg}}/10}} \\ &= \frac{A_1}{A_2} 10^{\left(P_{\mathrm{tx}}^{\mathrm{des}} - P_{\mathrm{tx}}^{\mathrm{agg}} + \phi^{\mathrm{agg}}\right)/10} \left(\frac{d_2^{\alpha_2}}{d_1^{\alpha_1}}\right),\end{aligned} \tag{3}$$

where A_1 and A_2 are the constants, α_1 and α_2 are the path loss exponents, and $P_{\mathrm{tx}}^{\mathrm{des}}$ and $P_{\mathrm{tx}}^{\mathrm{agg}}$ are the transmitted power from the desired and aggressor vehicles, respectively.

By transforming (3) at the dB scale, the SINR can be written as

$$\gamma = K + a_1 \ln\left(\frac{1}{d_1}\right) + a_2 \ln\left(d_2\right) \text{ in dB}, \tag{4}$$

where

$$K = 10\log_{10}\left(\frac{A_1}{A_2}\right) + P_{\mathrm{tx}}^{\mathrm{des}} - P_{\mathrm{tx}}^{\mathrm{agg}} + \phi^{\mathrm{agg}}, \tag{5}$$

$$a_1 = 10\alpha_1 \log_{10} e, \tag{6}$$

and

$$a_2 = 10\alpha_2 \log_{10} e. \tag{7}$$

The PDF of the SINR, denoted as f_Y, is derived in [16] as

$$f_Y(t) = \begin{cases} \dfrac{2D_1^{2a_1/a_2}}{(a_1+a_2)D_2^2} e^{2(t-K)/a_2}, & t < \ln\left(\dfrac{D_2^{a_2}}{D_1^{a_1}}\right) + K \\ \dfrac{2D_2^{2a_2/a_1}}{(a_1+a_2)D_1^2} e^{-2(t-K)/a_1}, & t \geq \ln\left(\dfrac{D_2^{a_2}}{D_1^{a_1}}\right) + K \end{cases}, \tag{8}$$

where D_1 and D_2 are the upper bounds of d_1 and d_2, respectively.

By applying the shadowing model between the desired transmitter and victim vehicle, (4) can be expressed in dB as:

$$\gamma = X + K + a_1 \ln\left(\frac{1}{d_1}\right) + a_2 \ln\left(d_2\right), \tag{9}$$

where X is a random component for the desired path shadowing.

The PDF of the shadowing model, which has a log normal distribution, is given by [38] as

$$f_X(x) = \frac{1}{\sqrt{2\pi\sigma^2}} \exp\left(-\frac{x^2}{2\sigma^2}\right), \quad -\infty < x < \infty, \tag{10}$$

where σ represents the standard deviation.

Considering the shadowing model, the PDF of the SINR f_Z can be derived as

$$
\begin{aligned}
f_Z(z) &= \int_{-\infty}^{\infty} f_X(x) f_Y(z-x)\,dx \\
&= \int_{-\infty}^{z-\ln\left(\frac{D_2^{a_2}}{D_1^{a_1}}\right)-K} \left\{ \frac{e^{-x^2/2\sigma^2}}{\sqrt{2\pi\sigma^2}} \frac{2D_2^{2a_2/a_1}}{(a_1+a_2)\,D_1^2} e^{\frac{-2(z-K-x)}{a_1}} \right\} dx \\
&+ \int_{z-\ln\left(\frac{D_2^{a_2}}{D_1^{a_1}}\right)-K}^{\infty} \left\{ \frac{e^{-x^2/2\sigma^2}}{\sqrt{2\pi\sigma^2}} \frac{2D_1^{2a_1/a_2}}{(a_1+a_2)\,D_2^2} e^{\frac{2(z-K-x)}{a_2}} \right\} dx \\
&= \frac{2D_2^{2a_2/a_1} e^{2\sigma^2/a_1^2}}{(a_1+a_2)\,D_1^2} e^{\frac{-2(z-K)}{a_1}} Q\left(\frac{1}{\sigma}\left(-c_p+\frac{2\sigma^2}{a_1}\right)\right) \\
&+ \frac{2D_1^{2a_1/a_2} e^{2\sigma^2/a_2^2}}{(a_1+a_2)\,D_2^2} e^{\frac{2(z-K)}{a_2}} Q\left(\frac{1}{\sigma}\left(c_p+\frac{2\sigma^2}{a_2}\right)\right)
\end{aligned} \tag{11}
$$

where

$$c_p = z - \ln\left(\frac{D_2^{a_2}}{D_1^{a_1}}\right) - K \tag{12}$$

and

$$Q(x) = \frac{1}{\sqrt{2\pi}} \int_x^{\infty} e^{\left(-\frac{u^2}{2}\right)} du. \tag{13}$$

4 | ANALYSIS ADJACENT CHANNEL INTERFERENCE

4.1 | Test scenarios and conditions

The V2X communication system parameters for the ACI analysis are shown in Table 1. The height of the vehicle antenna is based on the height of a passenger car. The output power of the V2X device in the vehicle is set as 23 dBm while including 7 dBi of the antenna gain, whereas the output power of the RSU is 29 dBm owing to a larger antenna gain of 13 dBi. For convenience of analysis, it is assumed that all communication devices are as listed in Table 1, regardless of the type of communication network.

The values of ACLR, ACS, and ACIR are listed in Table 2 according to the V2X communication system. The ACLR value is set based on an output power of 23 dBm, and the ACS values for a WAVE system are set as 22–29 to account for extreme cases of performance. We assume that the ACLR value is independent of the antenna gain. In this paper, WAVE and LTE are used as examples to obtain the ACIR values. The ACIR values obtained from both these communication systems are more valuable for an analysis.

TABLE 2 ACIR for the V2X system [40]

Aggressor	Victim	Aggressor ACLR (dBc)	Victim ACS (dB)	ACIR (dB)
WAVE	WAVE	26	22–29	20.6–24.5
LTE	WAVE	30	22–29	21.4–26.5
WAVE	LTE	26	33	25.2
LTE	LTE	30	33	28.2

TABLE 1 V2X system parameters [39]

Parameter	Unit	Value	Description
Thermal noise	dBm/Hz	−174	N/A
NF	dB	10	Noise figure
L_{imp}	dB	5	Implementation loss
G_{ant}	dBi	7, 13	Antenna gain
P_{tx}	dBm	23, 29	Tx equivalent isotropic radiated power
H_{veh}	m	1.5	Vehicle height
H_{rsu}	m	15	RSU height
f_c	GHz	5.9	Center frequency
BW	MHz	10	Channel bandwidth

The two-ray path loss model is used to obtain the channel constants (A_1, A_2) and exponent values (α_1, α_2) in (3) under the conditions listed in Table 1. The constant and exponent values of the channel are $10^{-4.2}$ and 2.2 for V2V, and $10^{-5.8}$ and 1.6 for I2V, respectively. The shadowing variance σ is set as 4 dB while considering a V2X outdoor environment.

As mentioned previously, the ACI scenario has two parts, namely (a) the aggressor V2V channel causes ACI in the victim V2V channel and (b) the aggressor V2V channel causes ACI in the victim I2V channel. Each scenario is composed of four test cases according to the combination of two V2X communication systems, as shown in Table 3. The communication distance varies from a few meters to a few kilometers depending on the use cases and modulations. In addition, the performance of the ACI depends on the ratio of the desired path distance to the distance from the aggressor, which is defined as D_r:

$$D_r = D_1/D_2. \tag{14}$$

TABLE 3 Test cases and conditions

Test case	Aggressor	Victim
V2V ACI as Figure 2 Condition: $1 < D_r < 10$, $P_{\text{tx}} = 23$ dBm		
TC1	WAVE	WAVE
TC2	LTE	WAVE
TC3	WAVE	LTE
TC4	LTE	LTE
V2V ACI as Figure 3 Condition: $2 < D_r < 20$, $P_{\text{tx}} = 23, 29$ dBm		
TC5	WAVE	WAVE
TC6	LTE	WAVE
TC7	WAVE	LTE
TC8	LTE	LTE

By considering the communication environment and service, in the V2V environment, for the range of D_r, it is assumed that the range of d_1 is between d_2 and 10 times d_2. However, in the I2V environment, the RSU antenna is usually installed on a road pole and tens of meters high, the minimum range of D_r is set as 2, and the maximum range of D_r is set as 20 in consideration of the wide communication range of the RSU. An output power of 29 dBm is used for the RSU to test the I2V ACI scenario from TC5 to TC8.

The PDFs of the SINR for the V2V and I2V ACI scenarios are plotted in Figures 5 and 6, respectively. The numerical results are obtained from the ACIR in Table 2. In the results of the V2V ACI scenario, as the value of D_r increases from 1 to 10, the SINR distributions are shifted by 20 dB. However, in the I2V ACI scenario, the distributions are shifted by 18 dB as the value of D_r changes from 2 to 20. It can be observed that the PDF in the I2V ACI scenario has a smaller SINR distribution with a higher probability density of 0.064 owing to the I2V channel constant and exponent values.

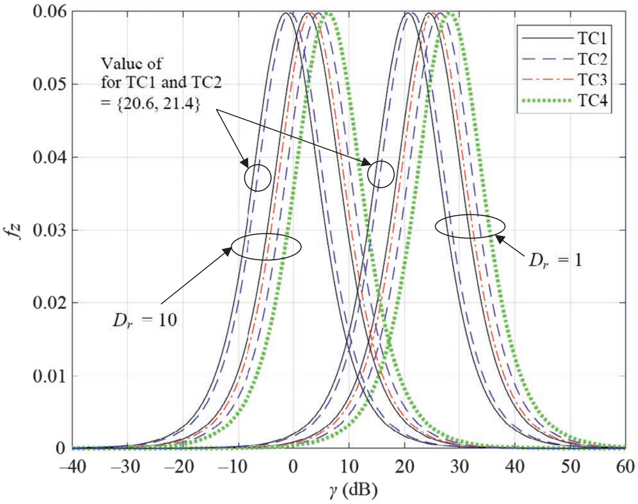

FIGURE 5 PDF for D_r range under V2V ACI scenario wherein $\sigma = 4$ dB

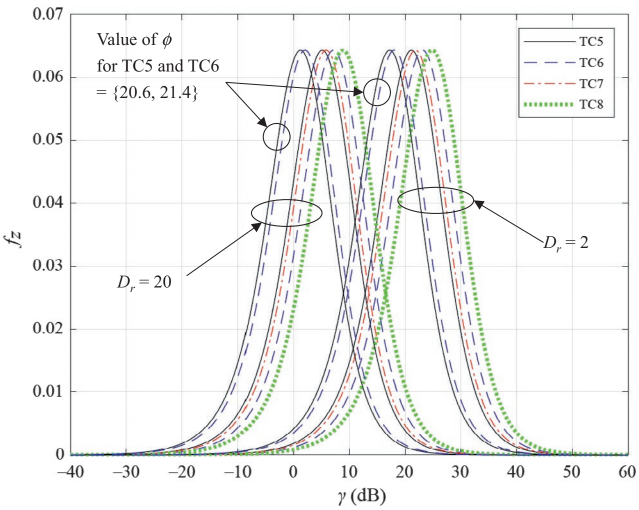

FIGURE 6 PDF for D_r range under I2V ACI scenario wherein $\sigma = 4$ dB

4.2 | Outage probability

The outage probability is derived from the receiver sensitivity. Considering the implementation loss, noise figure (NF), and thermal noise in Table 1, the receiver sensitivity is given by [41]

$$\begin{aligned} S_r &= -174\frac{\text{dBm}}{\text{Hz}} + 10\log_{10}\text{BW} + \text{NF} + \gamma + L_{\text{imp}}, \\ &= M + \gamma \end{aligned} \tag{15}$$

where

$$M = -174\frac{\text{dBm}}{\text{Hz}} + 10\log_{10}BW + NF + L_{\text{imp}}. \tag{16}$$

The value of M is computed as −89 dBm from Table 1. The PDF of the receiver sensitivity is derived from (11) as

$$\begin{aligned} f_S(s) &= f_Z(s-M) \\ &= \frac{2D_2^{2a_2/a_1} e^{2\sigma^2/a_1^2}}{(a_1+a_2)\,D_1^2} e^{\frac{-2(s-M-K)}{a_1}} Q\left(\frac{1}{\sigma}\left(-c_s + \frac{2\sigma^2}{a_1}\right)\right) \\ &+ \frac{2D_1^{2a_1/a_2} e^{2\sigma^2/a_2^2}}{(a_1+a_2)\,D_2^2} e^{\frac{2(s-M-K)}{a_2}} Q\left(\frac{1}{\sigma}\left(c_s + \frac{2\sigma^2}{a_2}\right)\right), \end{aligned} \tag{17}$$

where

$$c_s = s - \ln\left(\frac{D_2^{a_2}}{D_1^{a_1}}\right) - K - M. \tag{18}$$

Using (17), the cumulative distribution function (CDF) of the receiver sensitivity is obtained as

$$F_S(s) = P_r(S \le s) = \int_{-\infty}^{s} f_S(s)\,ds. \tag{19}$$

The CDF of the received signal is shown in Figures 7 and 8, where the vertical dotted line is the minimum receiver sensitivity based on the IEEE802.11p standard. For the V2V ACI scenario, TC1 through TC4 can receive a 64QAM signal of at least 70% for $D_r = 1$, and a signal of less than 4% for $D_r = 10$. They can also receive a QPSK signal of more than 95% for $D_r = 1$, and a signal of less than 40% for $D_r = 10$. As compared to the I2V ACI scenario, TC5 through TC8 can receive a 64QAM signal of more than 50% for $D_r = 2$, and a signal of less than 4% for $D_r = 20$. They can also receive a QPSK signal of more than 95% for $D_r = 2$, and a signal of less than 60% for $D_r = 20$.

4.3 | Packet error rate under fading channel

A Nakagami-*m* fast fading channel model is suitable for open environments such as a highway. A Rayleigh channel can be obtained under the conditions of a Nakagami channel with $m = 1$. Using Viterbi hard-decision decoding, the bit error rate equations for the mode of binary phase shift keying (BPSK) and N-ary quadrature amplitude modulation (QAM) are written in terms of the SINR per symbol, as described in [35]. We modified the equations for consistency in terms of the SINR of the received signal. Thus, the bit error probability for the BPSK can be written as:

$$p_b^{\mathrm{BPSK}}(\gamma)=\frac{1}{2}\left(1-\sqrt{\frac{\left(\gamma n_b B_W T_b a_g\right)}{1+\left(\gamma n_b B_W T_b a_g\right)}}\right). \tag{20}$$

In the same manner, the bit error probability for N-ary QAM can be obtained as

$$p_b^{N-\mathrm{QAM}}(\gamma) = 2\left(\frac{\sqrt{N}-1}{\sqrt{N}}\right)\left(\frac{1}{\log_2 N}\right)\sum_{i=1}^{\sqrt{N}/2}\left(1-\mu_i^{N-\mathrm{QAM}}(\gamma)\right) \tag{21}$$

where

$$\mu_i^{N-\mathrm{QAM}}(\gamma)=\sqrt{\frac{1.5\,(2i-1)^2\left(\gamma n_b B_W T_b a_g\right)}{N-1+1.5\,(2i-1)^2\left(\gamma n_b B_W T_b a_g\right)}}. \tag{22}$$

Using (20), the upper bound packet error rate (PER) in a Rayleigh fading channel is calculated for a packet length L, as described in [42], as

$$p_k^{\mathrm{mcs}}(\gamma)\le 1-\left(1-\sum_{d=d_{\mathrm{free}}}^{\infty} a_d\cdot p^{\mathrm{mcs}}(\gamma,d)\right)^L, \tag{23}$$

where

$$p^{\mathrm{mcs}}(\gamma,d) = \sum_{k=\frac{d+1}{2}}^{d}\binom{d}{k}\left(p_b^{\mathrm{mcs}}(\gamma)\right)^k\left(1-p_b^{\mathrm{mcs}}(\gamma)\right)^{d-k},\ d=\mathrm{odd} \tag{24}$$

or

$$\sum_{k=\frac{d}{2}+1}^{d}\binom{d}{k}\left(p_b^{\mathrm{mcs}}(\gamma)\right)^k\left(1-p_b^{\mathrm{mcs}}(\gamma)\right)^{d-k} + \frac{1}{2}\binom{d}{d/2}\left(p_b^{\mathrm{mcs}}(\gamma)\right)^{d/2}\left(1-p_b^{\mathrm{mcs}}(\gamma)\right)^{\frac{d}{2}},\ d=\mathrm{even} \tag{25}$$

The values of a_d and d_{free} are dependent on the convolutional encoder scheme, as shown in [43] and [44].

The average PER using the PDF can be calculated from (11) and (23) as

$$\begin{aligned}\bar{p}_k^{\mathrm{mcs}} &= \int_0^\infty p_k^{\mathrm{mcs}}(\gamma) f_\Gamma(\gamma)\,d\gamma \\ &= \int_0^\infty p_k^{\mathrm{mcs}}(\gamma)\, w_1 e^{\frac{-2(\gamma-K)}{a_1}} Q\left(\frac{1}{\sigma}\left(-w_3+\frac{2\sigma^2}{a_1}\right)\right)d\gamma \\ &\quad + \int_0^\infty p_k^{\mathrm{mcs}}(\gamma)\, w_2 e^{\frac{2(\gamma-K)}{a_2}} Q\left(\frac{1}{\sigma}\left(w_3+\frac{2\sigma^2}{a_2}\right)\right)d\gamma\end{aligned} \tag{26}$$

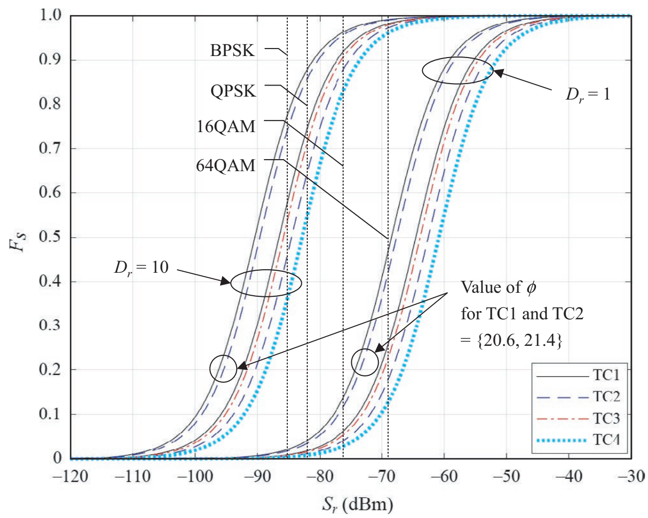

FIGURE 7 CDF for D_r range under V2V ACI scenario wherein NF and L_{imp} are 10 and 5 dB, respectively

where

$$w_1=\frac{2D_2^{2a_2/a_1}e^{2\sigma^2/a_1^2}}{\left(a_1+a_2\right)D_1^2}, \tag{27}$$

$$w_2=\frac{2D_1^{2a_1/a_2}e^{2\sigma^2/a_2^2}}{\left(a_1+a_2\right)D_2^2}, \tag{28}$$

$$w_3=\gamma-\ln\left(\frac{D_2^{a_2}}{D_1^{a_1}}\right)-K. \tag{29}$$

The average PER under a Rayleigh fading channel for the modulation and coding scheme (MCS) 3 is shown in Figures 9 and 10. TC1 through TC4 under the V2V ACI scenario can satisfy the requirement of a 10% PER with a range of D_r up to 3.3, 4.0, 3.5, and 4.9, respectively. The value of D_r is further

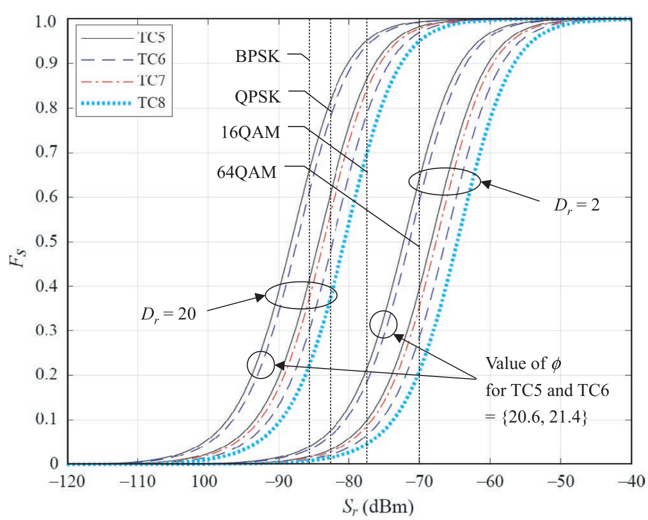

FIGURE 8 CDF for D_r range under I2V ACI scenario wherein NF and L_{imp} are 10 and 5 dB, respectively

reduced by 2.2 for TC1 and 2.5 for TC2 to obtain a 10% PER for the ACIR of 20.6 and 21.4, respectively. It was observed that the ACIR is required to be improved to 35 dB for a 10% PER requirement for TC2 with MCS 3. TC5 through TC8 in the I2V ACI scenario can satisfy the requirement of a 10% PER with a D_r range of up to 6.2, 8.2, 6.5, and 10.5, respectively. The value of D_r is further reduced by 3.4 for TC5 and 4.0 for TC6 to obtain a 10% PER for the ACIR of 20.6 and 21.4, respectively. It was observed that the ACIR is required to be improved up to 33 dB for a 10% PER requirement for TC6 with MCS 3. As compared to the V2V ACI scenario with the ACIR of 20.6 and 21.4, it is shown that the I2V ACI scenario is more sensitive to the PER performance owing to the larger degradation.

Among the eight test cases in Table 3, we have analyzed the cases wherein LTE is an aggressor and WAVE is a victim. In this interference environment, TC2 becomes a test case of V2V

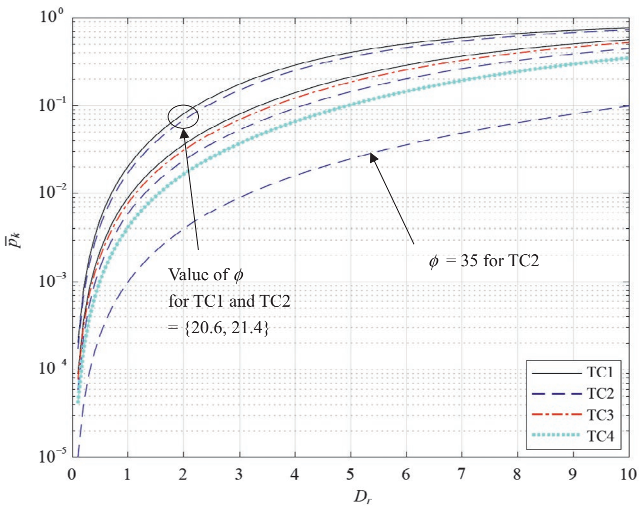

FIGURE 9 Average PER under a Rayleigh fading channel in V2V ACI scenario wherein L = 1,024 bytes and MCS 3

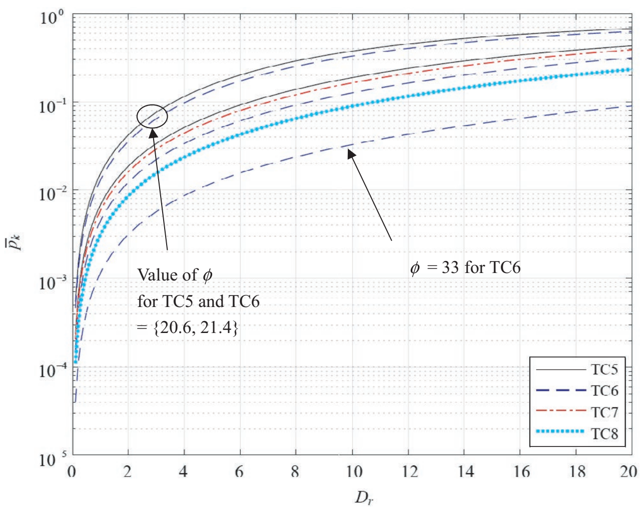

FIGURE 10 Average PER under a Rayleigh fading channel in the I2V ACI scenario wherein L = 1,024 bytes and MCS 3

and TC6 becomes a test case of I2V. In the V2V ACI scenario, {24.5, 26.5, 25.2, 28.2} listed in Table 2 are used as ACIR values for TC1 to TC4, respectively. In particular, for TC2, the result of ACIR 35 that satisfies a 10% PER at D_r = 10 was added. Similarly, in the I2V ACI scenario, {24.5, 26.5, 25.2, 28.2} listed in Table 2 are used as the ACIR values for TC5 to TC8, respectively. However, for TC6, the result of ACIR 33 that satisfies the 10% PER at D_r = 20 was added.

The average PER under a Rayleigh fading channel for TC2 and TC6 with different MCSs is shown in Figures 11 and 12, respectively, where two different ACIRs are used for comparison. As the MCS increases, the range of D_r satisfying a 10% PER is decreased. The PER performance does not match the MCS order owing to the difference in coding gain. When the ACIR is increased from 26.5 to 36.5 dB, in the V2V ACI scenario shown in Figure 11, MCS1 and MCS3 have a PER of less than 10% at D_r = 10. In the case of MCS 2, 4, 5, and 6, the range of the maximum D_r *satisfying* a 10% PER increases to 8.5, 7.3, 9.8, and 5.4, respectively. Similarly, in the I2V ACI scenario shown in Figure 12, MCS 1, 2, 3, and 5 show a PER of less than 10% even at D_r = 20. In the case of MCS 4 and 6, the maximum range of D_r satisfying a 10% PER increases to 18.5 and 12.5, respectively. However, a high MCS shows that a greater ACIR improvement is required to obtain a 10% PER.

4.4 | V2X throughput

Song and Choi [45]studied the maximum throughput for WAVE is computed for the different MCSs and packet sizes under error-free conditions. The V2X throughput under the ACI scenario can be obtained by considering the packet error rate as

$$\xi^{\text{mcs}} = \xi^{\text{mcs}}_{\text{max}} \times \left(1 - \bar{p}^{\text{mcs}}_k\right). \tag{30}$$

Under the same conditions, the maximum throughput of LTE is typically higher than that of WAVE owing to the better MAC efficiency of the frame structure of the former. However, to focus on the performance changes, in this paper we assume that LTE and WAVE have the same maximum throughput for the given MCS scheme. The average throughput in the V2V ACI and I2V ACI scenario under a Rayleigh fading channel is shown in Figures 13 and 14, respectively, where an MCS of 3 is used. The D_r point for a 10% throughput reduction is the same as the D_r point for a 10% PER reduction, as expected.

In the V2V ACI scenario of Figure 13, TC4 has a 10% throughput reduction at D_r = 5, whereas TC1 through TC3 have a 21%, 15%, and 19% throughput reduction, respectively. In particular, when an ACIR of 20.6 and 21.4 is applied, the throughput of TC1 and TC2 decrease by 40% and 36%, respectively. For the TC2 of interest, increasing the ACIR to 35 dB can improve the 10% throughput reduction point to D_r = 10. Similarly, in the I2V ACI scenario in Figure 14, TC8 has a 10% throughput reduction at D_r = 11, whereas TC5 through TC7 have a throughput

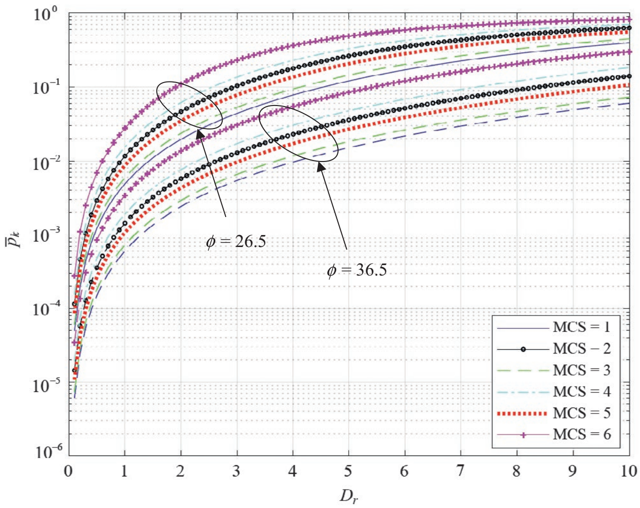

FIGURE 11 Average PER under a Rayleigh fading channel for TC2 under the V2V ACI scenario wherein $L = 1{,}024$ bytes

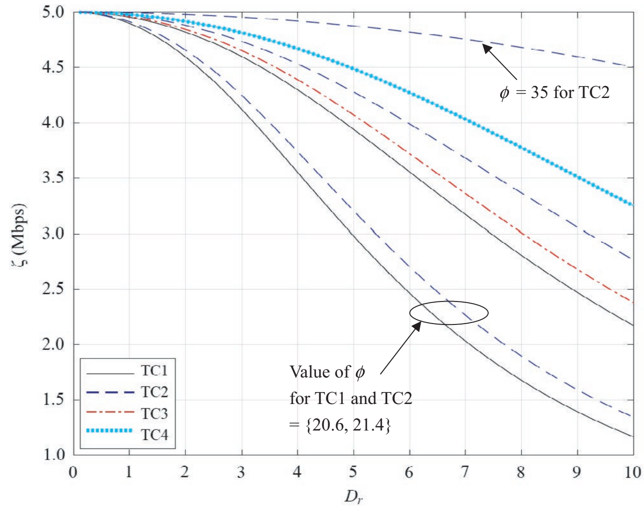

FIGURE 13 Throughput under a Rayleigh fading channel under the V2V ACI scenario wherein $L = 1{,}024$ bytes and for MCS 3

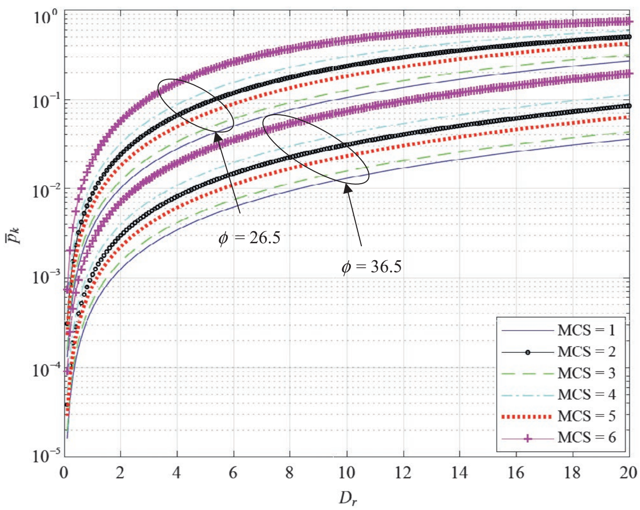

FIGURE 12 Average PER under a Rayleigh fading channel for TC6 under the I2V ACI scenario wherein $L = 1{,}024$ bytes

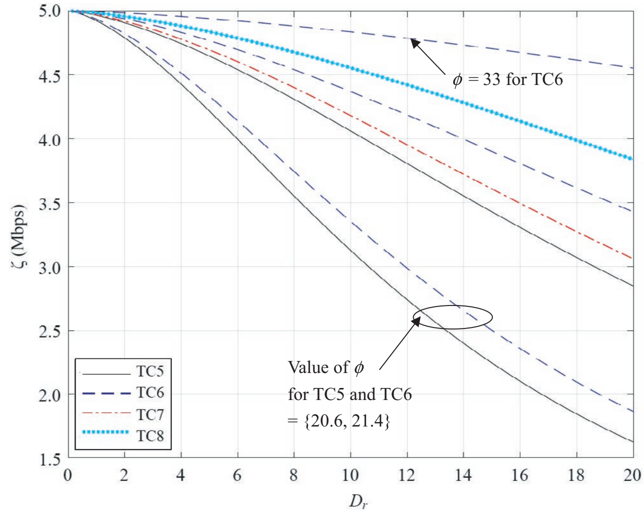

FIGURE 14 Throughput under a Rayleigh fading channel under the I2V ACI scenario wherein $L = 1{,}024$ bytes and for MCS 3

reduction of 21%, 15%, and 19%, respectively. In particular, when an ACIR of 20.6 and 21.4 is applied, the throughput of TC5 and TC6 is decreased by 42% and 36%, respectively. For the TC6 of interest, increasing the ACIR to 33 dB can improve the 10% throughput reduction point to $D_r = 20$.

The throughput under a Rayleigh fading channel for the different MCSs is shown in Figures 15 and 16. Furthermore, when D_r increases, the throughput decreases rapidly, particularly for a high MCS. In addition, it can be observed that the performance degradation slopes of MCSs 1, 3, and 5 are smoother than those of MCSs 2, 4, and 6 owing to the robustness against interference. The throughput performance indicated by the dashed line is obtained by adding an ACIR of 10 dB for the purpose of comparison. In the V2V ACI scenario of Figure 15, as the value of ACIR increases by 10 dB, the value of D_r with a 10% throughput reduction is improved from {4.5, 2.9, 4.1, 2.5, 3.4, 1.9} to {13, 8.4, 11.5, 7.3, 9.7, 5.4} for each MCS level. Similarly, in the I2V ACI scenario of Figure 16, the value of D_r with a 10% throughput reduction is improved from {9.6, 5.3, 8.5, 4.4, 6.5, 2.9} to {>20, 22, >20, 18.4, >20, 12.4} for each MCS level. This shows that the high MCS, especially MCS 6, requires a greater improvement in the ACIR to meet the 10% performance reduction condition.

5 | CONCLUSION

In this paper, the ACI performance for V2X systems was discussed to analyze the minimum requirements of the ACIR

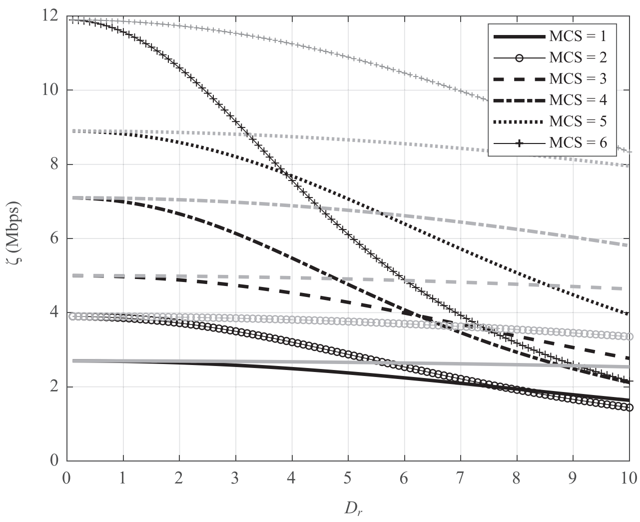

FIGURE 15 Throughput under a Rayleigh fading channel for TC2 under the V2V ACI scenario wherein $L = 1{,}024$ bytes

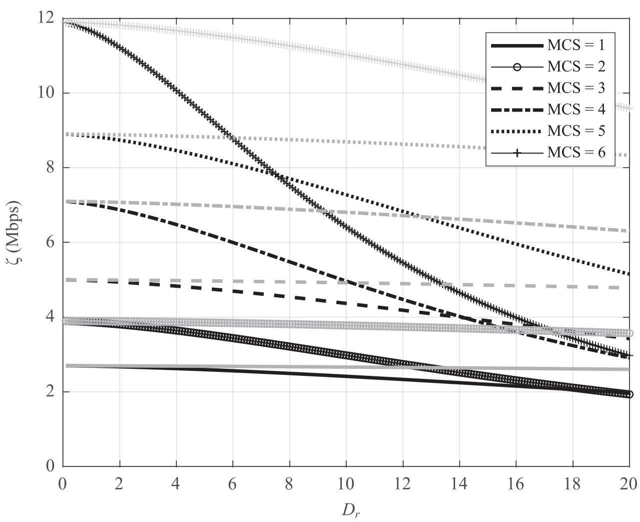

FIGURE 16 Throughput under a Rayleigh fading channel for TC6 under the I2V ACI scenario wherein $L = 1{,}024$ bytes

and the maximum ratio of the victim V2X coverage over the aggressor V2X coverage. Two different V2X scenarios are defined, including four test cases in each scenario according to the different combinations of communication systems and roles. The analysis of the ACI performance was performed as follows. First, the PDF of the SINR was derived, while taking into consideration the link distance for the desired and interfering path, the path loss characteristics, and the log normal shadowing effects. Second, the CDF of the receiver sensitivity was derived to analyze the outage probability under the given noise figure and implementation loss. Finally, a Nakagami-*m* fast fading channel was used to compute the PER. The average PER is obtained using the packet probability and the PDF of the SINR and then used for obtaining the V2X throughput. For the same D_r, the results obtained under the I2V ACI scenario (TC5 through TC8) outperform those obtained under the V2V ACI scenario (TC1 through TC4) owing to the better path loss characteristics and greater EIRP transmission power. The performance metric D_r is determined by considering the communication service ranges and is selected as 10 and 20 for the V2V and I2V ACI scenarios, respectively. The maximum allowed value of D_r under the V2V and I2V ACI scenarios is 5 with TC4 and 11 with TC8, respectively, to meet a 10% PER requirement when the MCS is 3. In the analysis of the PER and throughput with different MCSs, the 10% PER performance for MCS 6 is degraded by more than 2 and 3 times, respectively, under the V2V and I2V ACI scenarios as compared with MCS 1. The throughput performance decreases rapidly as D_r increases, particularly in the case of a high MCS. In addition, it is shown that the degradation slopes of MCSs 1, 3, and 5 are smoother than those of MCSs 2, 4, and 6 owing to the robustness against the interference. In this paper, it can be observed that the ACIR value of 28 dB or less does not satisfy the performances of D_r and PER. Under both the aforementioned scenarios, when MCS 3 is used, the ACIR value must be at least 35 dB to obtain a 10% PER performance. If the ACIR value is approximately 37 dB, the majority of the MCSs satisfy the performance criterion, but a high MCS, such as MCS 6 or above, requires a higher ACIR value of 40 dB.

ORCID

Yoo Seung Song https://orcid.org/0000-0003-1380-0755

REFERENCES

1. K. Aldana, U.S. *Department of Transportation Releases Policy on Automated Vehicle Development*, NHTSA, US Department of Transportation, 2013. Accessed Dec. 13, 2018. https://www.transportation.gov/briefing-room.
2. SAE J3016, *Taxonomy and definitions for terms related to driving automation systems for on-road motor vehicles*, SAE International, Warrendale, PA, USA, Sept. 2016.
3. 3GPP TR 22.886 v15.1.0, 3rd *generation partnership project; Technical specification group services and system aspects; Study on enhancement of 3GPP support for 5G V2X services (Release 15)*, Valbonne, France, Mar. 2017.
4. ETSI TR 102 638 v1.1.1, *Intelligent transport systems (ITS); Vehicular communications; Basic set of applications; Definitions*, Sophia Antipolis Cedex, France, June 2009.
5. ETSI 302 637-2 v1.3.1, *Intelligent transport systems (ITS); Vehicular communications; Basic set of application; Part2: Specification of cooperative awareness basic service*, Sophia Antipolis Cedex, France, Sept. 2014.
6. ETSI 302 637-3 v1.2.1, *Intelligent transport systems (ITS); Vehicular communications; Basic set of application; Part3: specification of decentralized environmental notification basic service*, Sophia Antipolis Cedex, France, Sept. 2014.

7. SAE J2735, *Dedicated short range communications (DSRC) message set dictionary*, SAE International, Warrendale, PA, USA, Nov. 2009.
8. Preliminary draft revision of recommendation ITU-R M.2084-0, *Radio interface standards of vehicle-to-vehicle and vehicle-to-infrastructure communications for Intelligent Transport Systems applications*, International Telecommunication Union, Sept. 2015.
9. IEEE802.11, *IEEE standard for information technology-telecommunication and information exchange between systems local and metropolitan area networks specific requirements Part11: Wireless LAN medium access control (MAC) and physical layer (PHY) specifications*, IEEE, Piscataway, NJ, USA, 2012.
10. IEEE1609.2, *IEEE standard for wireless access in vehicular environments-security services for applications and management messages*, IEEE, New York, NY, USA, 2016.
11. IEEE1609.3, *IEEE standard for wireless access in vehicular environments(WAVE) – networking services*, IEEE, New York, NY, USA, 2016.
12. IEEE1609.4, *IEEE standard for wireless access in vehicular environments (WAVE) – multi-channel operation, IEEE*, New York, NY, USA, 2016.
13. 3GPP TR 36.885 v14.0.0, *Study on LTE based V2X services (Release 14)*, Valbonne, France, June 2016.
14. Qualcomm, *Accelerating C-V2X commercialization*, Sept. 2017, Accessed Dec. 13, 2018. http://www.qualcomm.com
15. 5GAA (5G Automotive Association), *The case for cellular V2X for safety and cooperative driving*, Nov. 2016.
16. H.K. Son and C.Y. Kim, *Derivation of probability function of signal-to-interference-plus-noise ratio for the MS-to-MS interference analysis*, Scientific World J. **2013** (2013), 1–6.
17. J. Me et al., *A latency and reliability guaranteed resource allocation scheme for LTE V2V communication systems*, IEEE. Trans. Wireless Commun. **17** (2018), 3850–3860.
18. B.P. Tewari and S.C. Ghosh, *Combined power control and Partially overlapping channel assignment for interference mitigation in dense WLAN*, in Proc. IEEE Int. Conf. AINA, Taipei, Taiwan, May 27–29, 2017, pp. 646–653.
19. K. Xiong et al., *Mobile service amount based link scheduling for high-mobility cooperative vehicular networks*, IEEE Trans. Veh. Technol. **66** (2017), 9521–9533.
20. C. Campolo et al., *On the impact of adjacent channel interference in multi-channel VANETs*, in Proc. IEEE Int. Conf. Commun., Kuala Lumpur, Malaysia, May 23–27, 2016, pp. 1–7.
21. W.Y. Yeo, S.H. Moon, and J.H. Kim, *Uplink scheduling and adjacent channel coupling loss analysis for TD-LTE deployment*, Scientific World J. **2014** (2014), 1–15.
22. Y.P. Wang and K.H. Chang, *Adjacent channel interference reduction for M-WiMAX TDD and WCDMA FDD coexistence by utilizing beamforming in M-WiMAX TDD system*, IEICE Trans. Commun. **E93-B** (2010), no. 1, pp. 111–124.
23. K. Xiong et al., *A broad beamforming approach for high-mobility communications*, IEEE Trans. Veh. Technol. **66** (2017), no. 11, 10546–10550.
24. Y. Lu et al., *Optimal multi-cell coordinated beamforming for downlink high-speed railway communications*, IEEE Tran. Veh. Technol. **66** (2017), 9603–9608.
25. A.M. Voicu et al., *Analyzing Wi-Fi/LTE coexistence to demonstrate the value of risk-informed interference assessment*, in Proc. IEEE DySPAN, Piscataway, NJ, USA, Mar. 6–9, 2017, pp. 1–10.
26. A. Tekovic et al., *Interference analysis between mobile radio and digital terrestrial television in the digital dividend spectrum*, Radio Eng. **26** (2017), no. 1, 211–220.
27. G. Naik, J.S. Liu, and J.M. Park, *Coexistence of wireless technologies in the 5 GHz bands: a survey of existing solutions and a roadmap for future research*, IEEE Commun. Surveys Tutorials **20** (2018), no. 3, 1–22.
28. M.J. Kim et al., *Modeling of adjacent channel interference in heterogeneous wireless networks*, IEEE Commun. Lett. **17** (2013), no. 9, 1174–1777.
29. Y.K. Yoon and Y.J. Chong, *Outage performance and derivation due to adjacent channel interference*, in Proc. Int. Conf. Wireless Mobile Commun. (ICWMC), Seville, Spain, June 22–26, 2014, pp. 10–13.
30. R.W. Heath, M. Kountouris, and T. Bai, *Modeling heterogeneous network interference using poisson point processes*, IEEE Trans. Signal Process. **61** (2013), no. 16, 4114–4126.
31. S.P. Damodaran and M. Pazha, *Analysis of interference modeling and coexistence for next-generation LTE cellular systems*, in Proc. Int. Conf. Commun. Process. (ICCSP), Melmaruvathur, India, Apr. 2–4, 2015, pp. 1608–1611.
32. R. Lasowski et al., *Evaluation of adjacent channel interference in single radio vehicular Ad-Hoc networks*, in IEEE Consumer Commun. Netw. Conf. (CCNC), Las Vegas, NV, USA, Jan. 9–12, 2011, pp. 267–271.
33. V. Angelakis et al., *Adjacent channel interference in 802.11a is harmful: testbed validation of a simple quantification model*, IEEE Commun. Mag. **49** (2011), no. 3, 160–166.
34. A. Mishra et al., *Partially overlapped channels not considered harmful*, in Proc. Joint Int. Conf. Meas. Modeling Comput. Syst. (SIGMETRICS), Saint Malo, France, June 26–30, 2006, pp. 63–74.
35. A.M. Voicu, L. Simic, and M. Petrova, *Inter-technology coexistence in a spectrum commons: a case study of Wi-Fi and LTE in the 5-GHz unlicensed band*, IEEE J. Selected Areas Commun. **24** (2016), no. 11, 3062–3077.
36. D. Hu and S. Mao, Ad Hoc Networks: on co-channel and adjacent channel interference mitigation in cognitive radio networks, Elsevier Science Ltd, Amsterdam, Netherlands, 2013, pp. 1629–1640.
37. A.F. Molisch et al., *On pathloss models for adjacent-channel interference in cognitive whitespace systems*, in Proc. IEEE Int. Conf. Commun. Workshops (ICC), Kuala Lumpur, Malaysia, May 23–27, 2016, pp. 682–688.
38. G.R. Cooper and C.D. McGillem, *Probabilistic methods of signal and system analysis*, 3rd ed., Oxford University Press, NY, USA, 1998.
39. Y.S. Song and J.D. Choi, *V2X throughputs based on link budget analysis for 5.8GHz WAVE systems*, in Proc. IEEE ICTC Conf., Jeju, Rep. of Korea, Oct. 28–30, 2015, pp. 981–985.
40. 3GPP TR 36.889 V13.0.0, *Study on licensed-assisted access to unlicensed spectrum (Release 13)*, Nov. 2015.
41. C. Dou et al., *An analytical model for deriving receiver sensitivity and minimum transmit power in 802.11.6 wireless body area networks*, in Proc. IEEE MTT-S Int. Microw. Workshop Series RF Wireless Technol. Biomed. Healthcare Applicat., Taipei, Sept. 21–23, 2015, pp. 138–140.
42. M.K. Simon and M.S. Alouini, *Digital communication over fading channels*, Wiley-IEEE Press, Hoboken, NJ, USA, 2005, p. 24.

43. D. Haccoun and G. Begin, *High-rate punctured convolutional codes for viterbi and sequential decoding*, IEEE Trans. Commun. **37** (1989), no. 11, 1113–1125.
44. J. Conan, *The weight spectra of some short low-rate convolutional codes*, IEEE Trans. Commun. **32** (1984), no. 9, 1050–1053.
45. Y.S. Song and H.K. Choi, *Analysis of V2V broadcast performance limit for WAVE communication systems using two-ray path loss model*, ETRI J. **39** (2017), no. 2, 213–221.

AUTHOR BIOGRAPHIES

Yoo Seung Song is a principal researcher in the Autonomous Driving Intelligence Research Section at the Electronics and Telecommunications Research Institute (ETRI), Daejeon, Republic of Korea. He received his BS degree in electrical engineering from Changwon National University, Republic of Korea, in 1996, and MS and PhD degrees in electrical and computer engineering from Wichita State University, Kansas, USA, in 1998 and 2001, respectively. From 2001 to 2005, he was with the Media Lab. of Samsung Electronics, Suwon, Republic of Korea. Since joining ETRI in 2005, his work has been focused on next-generation wireless LAN (WLAN), 3D-ray tracing, WAVE, cooperative intelligent transport systems, and V2X communications.

Shin Kyung Lee is a principal researcher in the Autonomous Driving Intelligence Research Section at ETRI, Daejeon, Republic of Korea. She received her BS and MS degrees in computer science from Chonnam National University, Gwangju, Republic of Korea, in 1999 and 2001, respectively. Since joining ETRI in 2000, her work has been focused on network management systems, WAVE, and V2X communications.

Jeong Woo Lee received his BS and MS degrees in computer engineering from Sungkyunkwan University, Suwon, Republic of Korea, in 1999 and 2001, respectively. Since 2001, he has been with the Autonomous Driving Intelligence Research Section, Electronics and Telecommunications Research Institute, Daejeon, Republic of Korea, where he is now a principal researcher. His main research interests are autonomous vehicles, V2V/V2I communications, and simulators in vehicles.

Do Wook Kang received his BS and MS degrees in Electrical and Electronic Engineering form Donshin University, Republic of Korea, in 2002 and 2004, respectively. From 2004 to 2011, he worked for R&D Center, Fumate Co., Ltd. Deajeon, Republic of Korea. Since 2011, he has been with the ETRI, Deajeon, Republic of Korea, where he is now a senior engineer. His main research interests are WLAN, WAVE, and V2X Communications.

Kyoung Wook Min received his BS and MS degrees in computer engineering from Pusan National University, Republic of Korea, in 1996 and 1998, respectively. Since 2001, he has been a principal member of research staff with ETRI, Republic of Korea, and he is also working toward a PhD in computer engineering from Chungnam National University, Republic of Korea. His main research areas are navigation service, unmanned ground vehicle, and location-based service.